human hepatocytes in mice infected with each genotype after 2-week IFN-treatment (Fig. 4). These results suggest that the decrease in HCV is due to the direct anti-viral effect of IFN and not induced by liver cell damage. The difference in the virus titer and susceptibility to IFN are considered to be due to the characteristics of the genotypes.

4. Discussion

In this study, we established a reverse genetics system of HCV genotype 1a and 2a clones using human hepatocyte chimeric mice. The HCV genotype 2a clone, JFH-1, has remarkable features, i.e., infects cultured Huh7 cell line as well as establish infection in chimeric mouse [7]. It has been reported that HCV genotype 1a clone, H77-S, also infects Huh7 cell line and produces infectious virion [14]. In the present study, we intrahepatically inoculated genotype 1a infectious clone, CV-H77C. As reported in chimpanzee [13,15–17], we were able to establish genotype 1a infection using human hepatocyte chimeric mice. Using this technique, it is hoped that we can conduct further experiments in the future using genetically engineered HCV clones. Experiments using chimeric clone described by Lindenbach et al. [7] should also provide further information regarding the variable replication property of HCV genomes. Modifying genomes with nucleotide substitutions allowed examination of the functions of HCV peptides as we showed with HBV [12].

As reported recently by Kneteman et al. [10], the mouse model system is useful for evaluating the effect of anti-HCV drugs such as IFN, protease inhibitors and polymerase inhibitors. As we showed in this study, the response to IFN therapy varied according to HCV genotype. Further experiments are necessary to determine whether differences in response to IFN are due to the different replication ability (replication level of genotype 2a clone was slightly lower than that of genotype 1b, see Figs. 2 and 3) or differences in genotypes, as has been reported in clinical studies [18]. As we showed in this study (Fig. 4), there is no hepatocyte damage or inflammation in the liver of the infected chimeric mouse. Thus, this model is suitable for the study of mechanisms involved in HCV replication and IFN resistance.

The intrahepatic injection method used in this study simplified our experiments using genetically engineered virus. This is particularly important in studies of protease inhibitors and polymerase inhibitors because HCV will easily develop resistance against these small molecule agents.

Previous studies identified amino acid sequences that correlate with different susceptibilities of genotype 1b HCV against IFN therapy, namely, interferon sensitivity determining region [19] and the PKR-eIF2 phosphorylation homology domain [20,21]. To elucidate such issues, we are currently trying to establish genotype 1b infection system using the method described in this paper.

In summary, we showed in the present study the successful application of a genetically engineered HCV in human hepatocyte chimeric mice. Using this mouse model, we showed that genotypes 1a and 2a HCV clones exhibit different susceptibilities to IFN-alpha therapy. Our mouse model seems useful for the study of HCV virology and resistance of HCV against IFN and for the development of new anti-HCV therapy.

Acknowledgements: The authors thank Rie Akiyama, Kana Kunihiro and Kiyomi Toyota for their expert technical help, Dr. Robert H. Purcell and Dr. Jens Bukh for providing the full-length HCV cDNA clone of pCV-H77C. This study was supported in part by a Grant-in-Aid for Scientific Research from Japanese Ministry of labor, Health and Welfare.

References

[1] WHO. (1999) Global surveillance and control of hepatitis C. Report of a WHO Consultation organized in collaboration with the Viral Hepatitis Prevention Board, Antwerp, Belgium. J. Viral. Hepat. 6, 35–47.

[2] Kiyosawa, K., Sodeyama, T., Tanaka, E., Gibo, Y., Yoshizawa, K., Nakano, Y., Furuta, S., Akahane, Y., Nishioka, K. and Purcell, R.H. (1990) Interrelationship of blood transfusion, non-A, non-B hepatitis and hepatocellular carcinoma: analysis by detection of antibody to hepatitis C virus. Hepatology 12, 671–675.

[3] Niederau, C., Lange, S., Heintges, T., Erhardt, A., Buschkamp, M., Hurter, D., Nawrocki, M., Kruska, L., Hensel, F., Petry, W. and Haussinger, D. (1998) Prognosis of chronic hepatitis C: results of a large, prospective cohort study. Hepatology 28, 1687–1695.

[4] Fried, M.W., Shiffman, M.L., Reddy, K.R., Smith, C., Marinos, G., Goncales Jr., F.L., Haussinger, D., Diago, M., Carosi, G., Dhumeaux, D., Craxi, A., Lin, A., Hoffman, J. and Yu, J. (2002) Peginterferon alfa-2a plus ribavirin for chronic hepatitis C virus infection. N. Engl. J. Med. 347, 975–982.

[5] Zhong, J., Gastaminza, P., Cheng, G., Kapadia, S., Kato, T., Burton, D.R., Wieland, S.F., Uprichard, S.L., Wakita, T. and Chisari, F.V. (2005) Robust hepatitis C virus infection in vitro. Proc. Natl. Acad. Sci. USA 102, 9294–9299.

[6] Wakita, T., Pietschmann, T., Kato, T., Date, T., Miyamoto, M., Zhao, Z., Murthy, K., Habermann, A., Krausslich, H.G., Mizokami, M., Bartenschlager, R. and Liang, T.J. (2005) Production of infectious hepatitis C virus in tissue culture from a cloned viral genome. Nat. Med. 11, 791–796.

[7] Lindenbach, B.D., Meuleman, P., Ploss, A., Vanwolleghem, T., Syder, A.J., McKeating, J.A., Lanford, R.E., Feinstone, S.M., Major, M.E., Leroux-Roels, G. and Rice, C.M. (2006) Cell culture-grown hepatitis C virus is infectious in vivo and can be recultured in vitro. Proc. Natl. Acad. Sci. USA 103, 3805–3809.

[8] Shimizu, Y.K., Weiner, A.J., Rosenblatt, J., Wong, D.C., Shapiro, M., Popkin, T., Houghton, M., Alter, H.J. and Purcell, R.H. (1990) Early events in hepatitis C virus infection of chimpanzees. Proc. Natl. Acad. Sci. USA 87, 6441–6444.

[9] Mercer, D.F., Schiller, D.E., Elliott, J.F., Douglas, D.N., Hao, C., Rinfret, A., Addison, W.R., Fischer, K.P., Churchill, T.A., Lakey, J.R., Tyrrell, D.L. and Kneteman, N.M. (2001) Hepatitis C virus replication in mice with chimeric human livers. Nat. Med. 7, 927–933.

[10] Kneteman, N.M., Weiner, A.J., O'Connell, J., Collett, M., Gao, T., Aukerman, L., Kovelsky, R., Ni, Z.J., Zhu, Q., Hashash, A., Kline, J., His, B., Schiller, D., Douglas, D., Tyrrell, D.L. and Mercer, D.F. (2006) Anti-HCV therapies in chimeric scid-Alb/uPA mice parallel outcomes in human clinical application. Hepatology 43, 1346–1353.

[11] Tateno, C., Yoshizane, Y., Saito, N., Kataoka, M., Utoh, R., Yamasaki, C., Tachibana, A., Soeno, Y., Asahina, K., Hino, H., Asahara, T., Yokoi, T., Furukawa, T. and Yoshizato, K. (2004) Near completely humanized liver in mice shows human-type metabolic responses to drugs. Am. J. Pathol. 165, 901–912.

[12] Tsuge, M., Hiraga, N., Takaishi, H., Noguchi, C., Oga, H., Imamura, M., Takahashi, S., Iwao, E., Fujimoto, Y., Ochi, H., Chayama, K., Tateno, C. and Yoshizato, K. (2005) Infection of human hepatocyte chimeric mouse with genetically engineered hepatitis B virus. Hepatology 42, 1046–1054.

[13] Yanagi, M., Purcell, R.H., Emerson, S.U. and Bukh, J. (1997) Transcripts from a single full-length cDNA clone of hepatitis C virus are infectious when directly transfected into the liver of a chimpanzee. Proc. Natl. Acad. Sci. USA 94, 8738–8743.

[14] Yi, M., Villanueva, R.A., Thomas, D.L., Wakita, T. and Lemon, S.M. (2006) Production of infectious genotype 1a hepatitis C virus (Hutchinson strain) in cultured human hepatoma cells. Proc. Natl. Acad. Sci. USA 103, 2310–2315.
[15] Kolykhalov, A.A., Agapov, E.V., Blight, K.J., Mihalik, K., Feinstone, S.M. and Rice, C.M. (1997) Transmission of hepatitis C by intrahepatic inoculation with transcribed RNA. Science 277, 570–574.
[16] Yanagi, M., StClaire, M., Emerson, S.U., Purcell, R.H. and Bukh, J. (1999) In vivo analysis of the 3′ untranslated region of the hepatitis C virus after in vitro mutagenesis of an infectious cDNA clone. Proc. Natl. Acad. Sci. USA 96, 2291–2295.
[17] Beard, M.R., Abell, G., Honda, M., Carroll, A., Gartland, M., Clarke, B., Suzuki, K., Lanford, R., Sangar, D.V. and Lemon, S.M. (1999) An infectious molecular clone of a Japanese genotype 1b hepatitis C virus. Hepatology 30, 316–324.
[18] McHutchison, J.G., Gordon, S.C., Schiff, E.R., Shiffman, M.L., Lee, W.M., Rustgi, V.K., Goodman, Z.D., Ling, M.H., Cort, S. and Albrecht, J.K. (1998) Interferon alfa-2b alone or in combination with ribavirin as initial treatment for chronic hepatitis C. Hepatitis Interventional Therapy Group. N. Engl. J. Med. 339, 1485–1492.
[19] Enomoto, N., Sakuma, I., Asahina, Y., Kurosaki, M., Murakami, T., Yamamoto, C., Ogura, Y., Izumi, N., Marumo, F. and Sato, C. (1996) Mutations in the non-structural protein 5A gene and response to interferon in patients with chronic hepatitis C virus 1b infection. N. Engl. J. Med. 334, 77–81.
[20] Taylor, D.R., Shi, S.T., Romano, P.R., Barber, G.N. and Lai, M.M. (1999) Inhibition of the interferon-inducible protein kinase PKR by HCV E2 protein. Science 285, 107–110.
[21] Chayama, K., Suzuki, F., Tsubota, A., Kobayashi, M., Arase, Y., Saitoh, S., Suzuki, Y., Murashima, N., Ikeda, K., Takahashi, N., Kinoshita, M. and Kumada, H. (2000) Association of amino acid sequence in the PKR-eIF2 phosphorylation homology domain and response to interferon therapy. Hepatology 32, 1138–1144.

Expression Profiling of Peripheral-Blood Mononuclear Cells from Patients with Chronic Hepatitis C Undergoing Interferon Therapy

Makoto Tateno,[1] Masao Honda,[1] Takashi Kawamura,[2] Hiroyuki Honda,[2] and Shuichi Kaneko[1]

[1]Department of Cancer Gene Regulation, Kanazawa University Graduate School of Medical Science, Kanazawa, and [2]Department of Biotechnology, School of Engineering, Nagoya University, Nagoya, Japan

Background. Interferon (IFN) is now the standard treatment for chronic hepatitis C (CH-C); however, treatment efficacy is unpredictable before IFN therapy is started.

Methods. We investigated the gene-expression profiles of peripheral-blood mononuclear cells (PBMCs) from patients with CH-C showing different responses to IFN. Gene-expression profiles of PBMCs were analyzed in 21 patients with CH-C treated with IFN alone or in combination with ribavirin as well as in 6 healthy volunteers. Serial changes in the gene-expression profiles of PBMCs from individual patients were evaluated before treatment, 2 weeks after the start of IFN therapy, and 6 months after the completion of IFN therapy.

Results. Interestingly, the gene-expression profiles of PBMCs from patients with CH-C and healthy volunteers differed substantially; early T cell–activation antigen CD69 was significantly up-regulated in patients with CH-C, but immune-related molecules such as chemokine (C-C motif) receptor 2 and interleukin 7 receptor were significantly down-regulated. Selected combinations of expressed genes obtained before treatment and during IFN therapy by use of a fuzzy neural network combined with the SWEEP operator method predicted the outcome of IFN therapy with peak accuracies of 91.0% and 90.2%, respectively.

Conclusions. These findings suggest that the gene-expression profiles of PBMCs from patients with CH-C may be useful biomarkers for IFN therapy.

Although interferon (IFN) is currently the standard treatment for patients with chronic hepatitis C (CH-C), only 30%–40% of patients completely eliminate the virus, even after effective IFN and ribavirin combination therapy [1–3]. The mechanism of viral persistence during IFN treatment remains to be clarified. It has been reported that several clinical factors, such as viral load, genotype, degree of fibrosis, and expression of type I IFN receptors, are useful predictive factors for the outcome of IFN therapy [4–6]; however, precise prediction is not possible at present.

Type I IFN, such as IFN-α and IFN-β, plays an important role in innate immunity against viral infections by suppressing viral replication [7, 8]. However, the biological activities of IFN have not been fully elucidated. In viral infections such as measles, the number of peripheral lymphocytes generally decreases. It has also been reported that infection of dendritic cells and other immunocompetent cells is involved in exacerbated disease states and persistent infection [9]. Hence, it may be possible to assess disease state and severity by examining peripheral-blood mononuclear cells (PBMCs) from infected individuals. PBMCs include lymphocytes and monocytes, which play the most important roles in the immunological response to viral infection.

In the present study, we investigated the gene-expression profiles of PBMCs from patients with CH-C and healthy volunteers by use of cDNA microarray techniques [10–16]. By determining the gene-expression profiles of PBMCs from patients with CH-C receiving IFN therapy, we also clarified the differences in the PBMC gene-expression profiles between patients

Received 30 May 2006; accepted 23 August 2006; electronically published 13 December 2006.

Potential conflicts of interest: none reported.

Reprints or correspondence: Shuichi Kaneko, Dept. of Cancer Gene Regulation, Kanazawa University Graduate School of Medical Science, 13-1, Takara-Machi, Kanazawa 920-8641, Japan (skaneko@medf.m.kanazawa-u.ac.jp).

The Journal of Infectious Diseases 2007;195:255–67

0022-1899/2007/19502-0014$15.00

Table 1. Clinical characteristics of patients and responses to interferon (IFN) therapy.

Group, patient (sex, age in years)	ALT level, IU/L	Histology score[a]	Serotype	IFN therapy	Response	Serum HCV RNA level, kIU/mL			PBMC HCV RNA at 2 weeks
						Before	2 weeks	6 months	
Group A									
1 (M, 46)	31	F1/A1	2	Mono	CR	23	<0.5	<0.5	−
2 (F, 47)	40	F1/A1	2	Mono	CR	416	<0.5	<0.5	+
3 (M, 71)	59	F4/A2	1	Mono	CR	42.3	2.2	<0.5	−
4 (M, 55)	19	F4/A2	2	Mono	CR	1.3	<0.5	<0.5	−
5 (M, 54)	30	F2/A1	1	Mono	BR	620	ND	>850	ND
6 (F, 43)	46	F2/A1	1	Mono	BR	160	<0.5	611	+
7 (M, 58)	236	F1-2/A1	NA	Mono	BR	360	<0.5	620	−
8 (M, 60)	114	F3/A2	2	Mono	BR	770	<0.5	2200	−
9 (M, 62)	70	F2/A1	1	Mono	NR	130	130	350	+
10 (M, 42)	59	F2/A1	1	Mono	NR	800	7.2	190	−
11 (F, 62)	138	F2-3/A2	2	Mono	NR	650	183	1400	+
12 (M, 49)	48	F2/A2	2	Mono	NR	330	<0.5	69.5	−
13 (F, 56)	104	F1/A1	1	Mono	NR	751	<0.5	610	−
Group B									
14 (M, 49)	69	F3/A2	1	Combination	CR	>850	ND	<0.5	ND
15 (M, 50)	35	F1/A2	1	Combination	CR	475	<0.5	<0.5	ND
16 (M, 44)	106	F2/A2	1	Combination	NR	325	68.8	82.6	ND
17 (M, 56)	30	F2/A1	1	Combination	CR	91	<0.5	<0.5	ND
18 (F, 39)	47	F1/A1	1	Combination	CR	>850	0.7	<0.5	ND
19 (F, 64)	117	F2/A1	1	Combination	NR	484	0.8	>850	ND
20 (M, 66)	31	F2/A1	1	Combination	NR	>850	390	1300	ND
21 (F, 62)	103	F3/A2	1	Combination	NR	820	270	1200	ND

NOTE. +, positive; −, negative; ALT, alanine aminotransferase; BR, biochemical responder; CR, complete responder; F, female; M, male; NA, not applicable; ND, not detected; NR, nonresponder; PBMC, peripheral-blood mononuclear cell.

[a] Grading and staging of chronic hepatitis were histologically assessed according to the method of Desmet et al. [17], as described in the text.

with CH-C who responded to IFN therapy (complete responders [CRs]) and those who did not (nonresponders [NRs]).

SUBJECTS, MATERIALS, AND METHODS

Patients. Subjects were 21 patients with CH-C and 7 patients who showed no clinical signs of hepatitis at Kanazawa University Hospital, Japan, between 1999 and 2001. To 13 patients with CH-C (group A), 6 million IUs of IFN-α2b was administered every day for 2 weeks and then 3 times weekly for 22 weeks. To 8 patients with CH-C (group B), IFN-α2b was administered in the same fashion, and ribavirin was administered concomitantly (600 mg for ≤60 kg of body weight, 800 mg for >60 and ≤80 kg of body weight, and 1000 mg for >80 kg of body weight). The 6 age- and sex-matched healthy volunteers were seronegative for either hepatitis B surface antigen or hepatitis C virus (HCV) antibody and had liver function values within normal limits. Eight CRs (negative HCV RNA for >6 months), 4 biochemical responders (BRs; normal serum alanine aminotransferase [ALT] levels for >6 months and positive serum HCV RNA), and 9 NRs to IFN therapy were enrolled. After informed consent was obtained from patients, peripheral-blood samples were collected before the start of IFN therapy, at 2 weeks into treatment, and at 6 months after the completion of treatment. PBMCs were then isolated from whole blood and stored in liquid nitrogen until use. Grading and staging of chronic hepatitis were histologically assessed according to the method of Desmet et al. [17]. Clinical characteristics, such as sex, age, ALT levels, degree of histological activity or staging, HCV RNA load and HCV serotype, did not differ significantly among the groups (table 1).

Virological assessment. The amount of HCV RNA was assayed by the Amplicor Monitor Test (Roche Molecular Systems). HCV was classified by a serologic genotyping assay that has been shown to be specific and sensitive for determining HCV genome subtype [18].

Preparation of cDNA microarray slides. Most cDNA clones used in the present study were obtained from IMAGE Consortium libraries through their distributor, Research Genetics, as described elsewhere [19–24]. In addition to these clones, we included clones to monitor IFN signaling. The newly constructed cDNA microarray slide (Kanazawa IFN chip; version 1.0) comprised 400 representative IFN signaling–related

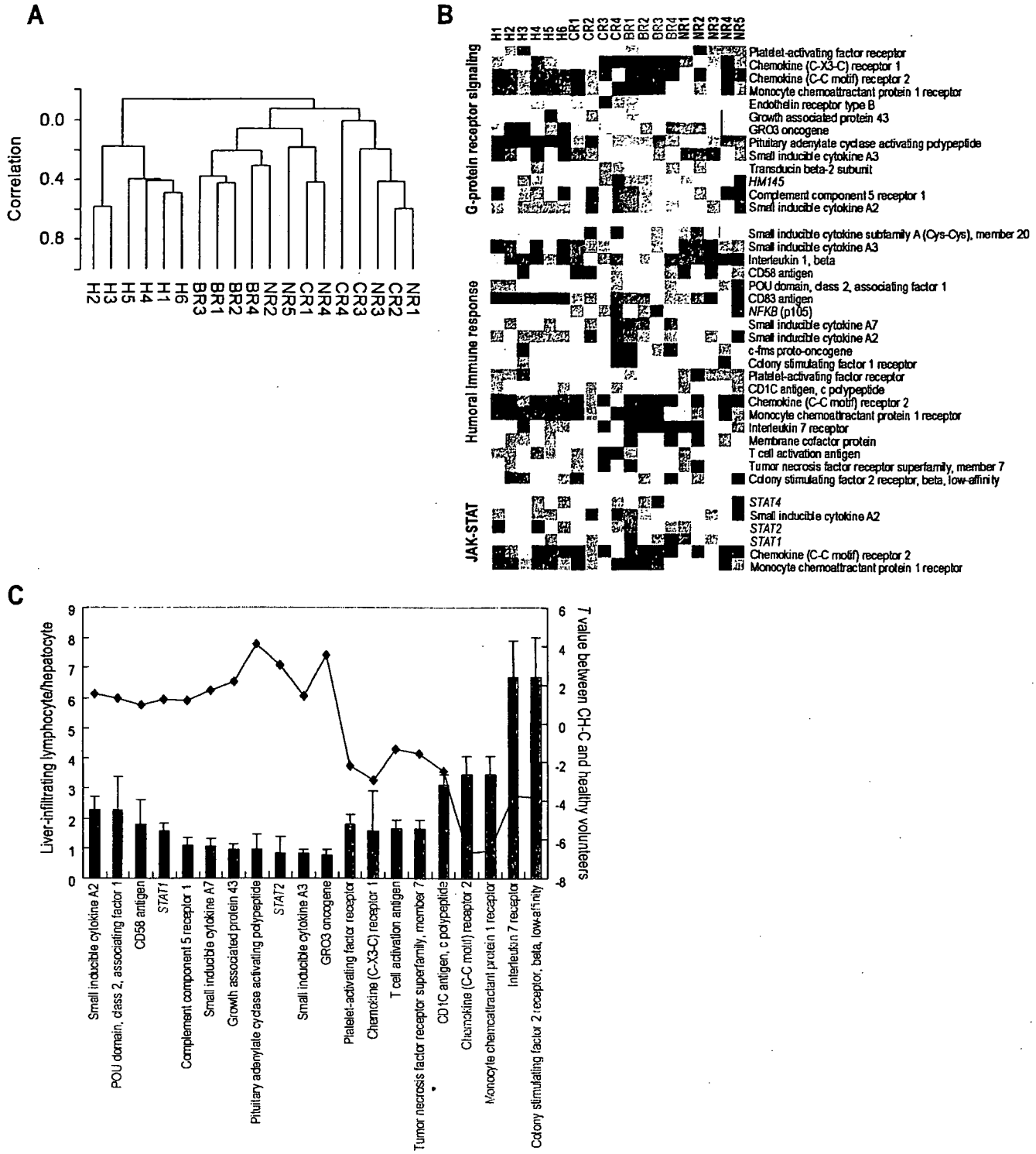

Figure 1. *A,* Hierarchical clustering analysis of gene-expression profiles of peripheral-blood mononuclear cell (PBMC) samples from 13 patients with chronic hepatitis C (CH-C; complete responders [CRs] 1–4, biochemical responders [BRs] 1–4, and nonresponders [NRs] 1–5) and 6 healthy volunteers (H1–H6) among 1305 tested genes before the start of interferon (IFN) therapy, performed using BRB-ArrayTools software. The dendrogram indicates the order in which patients were grouped on the basis of similarities in their gene-expression patterns. *B,* One-way clustering analysis of gene-expression profiles of PBMCs before the start of IFN therapy, using differentially expressed genes in the Janus kinase signal transducer and activation of transcription (JAK-STAT) cascade, humoral immune response, and G protein–coupled receptor protein signaling pathway. Gene cluster data are presented graphically as colored images; red indicates up-regulated genes, and blue indicates down-regulated genes. *C,* Bar graph indicating gene expression in liver-infiltrating lymphocytes relative to that in hepatocytes *(left axis),* and line graph indicating the *T* values for class-prediction analysis between patients with CH-C and healthy volunteers *(right axis).* Genes with increased expression in the liver *(red)* tended to be expressed at lower levels in PBMCs, and genes with decreased expression in the liver *(blue)* tended to be expressed at higher levels in PBMCs.

Table 2. Representative up- or down-regulated genes in patients with chronic hepatitis C, compared with that in healthy volunteers.

Category, gene name	Ratio	*T*	*P*	GenBank accession no.	Gene annotation
Up-regulated					
CD83 antigen (activated B lymphocytes, immunoglobulin superfamily)	3.60	4.26	.00125	NM_004233	Defense response
Thrombospondin 1	3.29	5.19	.00014	NM_003246	Endopeptidase inhibitor activity
CD69 antigen (p60, early T cell–activation antigen)	2.87	5.55	.00001	NM_001781	Transmembrane receptor activity
Regulator of G protein signaling 1	2.33	4.31	.00029	NM_002922	Signal transducer activity
Pituitary adenylate cyclase–activating polypeptide	2.01	4.12	.00046	NM_001117	Neuropeptide hormone activity
Nicotinamide N-methyltransferase	1.99	5.29	.00003	NM_006169	Methyltransferase activity
Clone rasi-1 matrix metalloproteinase RASI-1	1.70	4.56	.00019	NM_002429	Hydrolase activity
VASP, exons 4–13	1.68	4.35	.00026	NM_003370	Actin binding
Xeroderma pigmentosum, complementation group A	1.63	3.86	.00085	NM_000380	Damaged DNA binding
Urokinase-type plasminogen activator receptor; GPI-anchored form precursor *(UPAR)*; monocyte-activation antigen Mo3; CD87 antigen	1.53	4.41	.00023	NM_002659	Protein binding
Down-regulated					
Chemokine (C-C motif) receptor 2	0.35	−6.69	.00000	NM_000647	C-C chemokine receptor activity
Interleukin 7 receptor	0.47	−3.69	.00129	NM_002185	Antigen binding
Annexin II (lipocortin II)	0.49	−4.86	.00007	NM_004039	Calcium ion binding
Colony stimulating factor 2 receptor β, low-affinity (granulocyte-macrophage)	0.52	−3.85	.00088	NM_000395	Interleukin 3 receptor activity
Cytoplasmic dynein light chain	0.53	−4.12	.00046	NM_003746	Enzyme inhibitor activity
Ribosomal protein L13a	0.55	−3.94	.00070	X56932	Structural constituent of ribosome
Ikaros/LyF-1 homolog	0.56	−4.30	.00029	NM_006060	DNA binding
Chaperonin-containing TCP1, subunit 4 (Δ)	0.56	−4.60	.00014	NM_006430	Unfolded protein binding
Eosinophil Charcot-Leyden crystal (CLC) protein (lysophospholipase)	0.57	−3.73	.00116	NM_001828	Hydrolase activity
Myeloid cell nuclear differentiation antigen	0.57	−3.66	.00138	M81750	DNA binding
Ribosomal protein S16	0.59	−3.84	.00091	M60854	Structural constituent of ribosome
FK506-binding protein 4 (59 kDa)	0.62	−4.28	.00030	NM_002014	Isomerase activity
Transforming growth factor β receptor IIB	0.62	−3.87	.00082	NM_003242	Type II transforming growth factor β receptor activity
Ribosomal protein L3	0.62	−3.80	.00099	X73460	Structural constituent of ribosome
KIAA0053	0.63	−5.73	.00001	D29642.1	GTPase activator activity
Peptidylprolyl isomerase D (cyclophilin D)	0.65	−4.71	.00011	NM_005038	FK506 binding
Citrate synthase	0.66	−5.54	.00001	NM_004077	Transferase activity
FADD	0.66	−3.72	.00119	NM_003824	Protein binding
C-myc oncogene	0.66	−3.84	.00089	NM_002467	Transcription factor activity
Interferon regulatory factor 2	0.66	−3.60	.00159	NM_002199	RNA polymerase II transcription factor activity
Intercellular adhesion molecule 3	0.66	−4.30	.00029	NM_002162	Protein binding

Table 3. Gene ontology (GO) comparison to discriminate between patients with chronic hepatitis C and healthy volunteers.

GO category	GO description	Genes, no.	*P* LS permutation	*P* KS permutation
7259	JAK-STAT cascade	6	.00167	.17913
6959	Humoral immune response	25	.00303	.03114
7186	G protein–coupled receptor protein signaling pathway	18	.00348	.17617

NOTE. JAK-STAT, Janus kinase signal transducer and activation of transcription; KS, Kolmogorov-Smirnov; LS, least squares.

genes, 200 receptor- and cell adhesion–related genes, 160 apoptosis- and cell cycle–related genes, 150 transcription factors, 120 stress-response genes, and 275 other functional genes.

RNA isolation and antisense RNA amplification. Total RNA from PBMCs was isolated using Micro RNA Isolation Kits (Stratagene), and antisense RNA (aRNA) was amplified as described elsewhere [20, 22, 24]. The quality and degradation of isolated RNA were estimated after electrophoresis using an Agilent 2001 bioanalyzer. The references used for each microarray analysis were aRNA samples prepared from PBMCs obtained from a healthy volunteer. Microarray hybridization was performed as described elsewhere [19–24], and each hybridization was repeated for all samples.

Gene-expression profiles of liver-infiltrating lymphocytes in

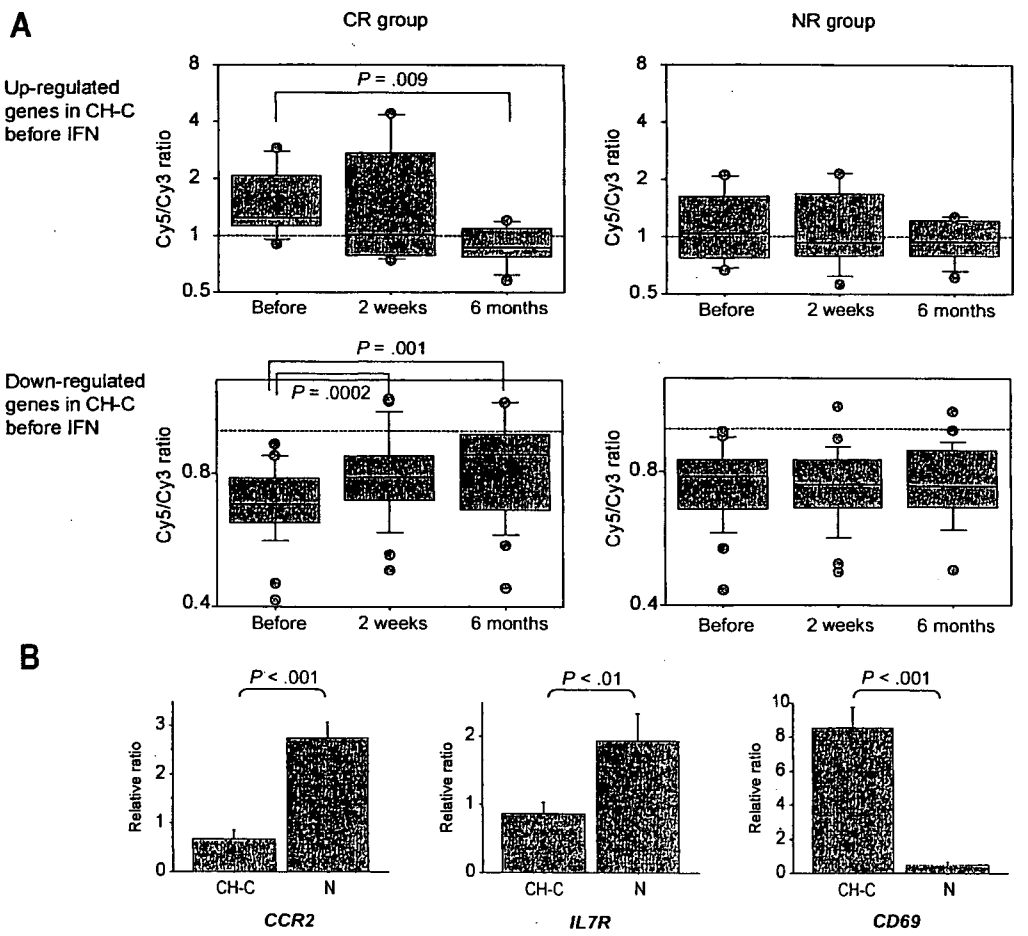

Figure 2. *A*, Changes in gene-expression profiles over the course of interferon (IFN) therapy (as shown in table 2) distinguishing patients with chronic hepatitis C (CH-C) from healthy volunteers before the start of IFN therapy. Box charts show average rates of change in relation to healthy volunteers as index functions. *B*, Real-time polymerase chain reaction data for *CCR2* and *IL7R*, which were down-regulated (as determined on the basis of microarray data) in patients with CH-C before the start of IFN therapy, and *CD69*, which was up-regulated in patients with CH-C.

patients with CH-C were investigated by laser-capture microdissection (LCM). Infiltrated lymphoid cells in the portal area and hepatocytes in liver-biopsy specimens obtained from 8 patients with CH-C were isolated by LCM. After 2 rounds of total RNA amplification, the gene expression in infiltrated lymphoid cells was compared with that in hepatocytes [25]. Optimal conditions for LCM and reproducibility of data were assessed repeatedly [24, 25]. Some of these data were used for the analysis of genes expression.

Image analysis and data processing. Quantitative assessment of signals on the slides was performed using a ScanArray 5000 device (General Scanning), followed by image analysis using QuantArray software (version 2.0; General Scanning).

Hierarchical clustering of gene expression in patients was performed using BRB-ArrayTools software (version 3.3.0; available at: http://linus.nci.nih.gov/BRB-ArrayTools.html). Filtered data were log transformed, normalized, centered, and applied to the average linkage clustering with centered correlation. BRB-ArrayTools include class comparison and class prediction tools based on univariate *F* tests to identify genes differentially expressed between predefined clinical groups. The permutation distribution of the *F* statistic, based on 2000 random permutations, was also used to confirm statistical significance. $P < .05$, as well as >1.5-fold differences in gene expression, were considered to be significant. A gene ontology (GO) comparison tool provides a list that has more genes differentially expressed and is coordinately regulated among predefined clinical groups than expected by chance and enables findings among biologically related genes to reinforce one another. Fisher and Kolmogorov-Smirnov tests were performed for GO comparison ($P < .005$) (BRB-ArrayTools).

Changes in gene expression in patients receiving IFN therapy were classified on the basis of self-organizing maps (GeneCluster software; version 2.0; available at: http://www.broad.mit.edu/cancer/software/genecluster2/gc2.html).

To identify class predictor genes for IFN therapy, projective adaptive resonance theory (PART) was used as a screening method for cDNA microarray data; unlike conventional clustering methods, PART enables the elimination of nonspecific dimensions for clustering from high-dimensional data [28–30]. From the genes extracted by PART, class predictor genes were selected using a fuzzy neural network (FNN) combined with the SWEEP operator method (FNN-SWEEP method). An FNN model with 1 input unit was initially created. Expression data for genes from data sets for patients with CH-C were entered into the FNN model, and the weight parameter was determined by the SWEEP operator method. We repeated this procedure for all genes to construct a model for each gene. The 10 genes with the highest accuracy levels were selected as the "first gene." The parameter increasing method was then applied. Having the first gene fixed, we used a similar method to select the second gene, which gave the highest accuracy in combination with the first gene. Having the first gene and the second gene fixed, we selected the third gene. For validation of this model, we performed leave-one-out cross-validation (LOOCV); we left out 1 test sample and used the remaining 12 samples as training samples. We created 13 such sets. The FNN model was built up for 12 test samples, and the accuracy of training and test samples was calculated.

Real-time quantitative reverse-transcription polymerase chain reaction (RT-PCR). Quantitation of chemokine (C-C motif) receptor 2 *(CCR2), CD69,* and interleukin 7 receptor *(IL7R)* RNA expression was performed using the TaqMan real-time PCR assay (ABI PRISM 7700 Sequence Detection System; PE Applied Biosystems), as described elsewhere [22, 23].

Statistical analysis. All data are expressed as mean ± SE values. One-way analysis of variance by the Bonferroni method or Student's *t* test was used to determine the significance of differences in clinical characteristics between patients in this study. $P < .05$ was considered to be significant.

RESULTS

cDNA microarray analysis of expression profiles of PBMCs from patients with CH-C. We initially compared the PBMC

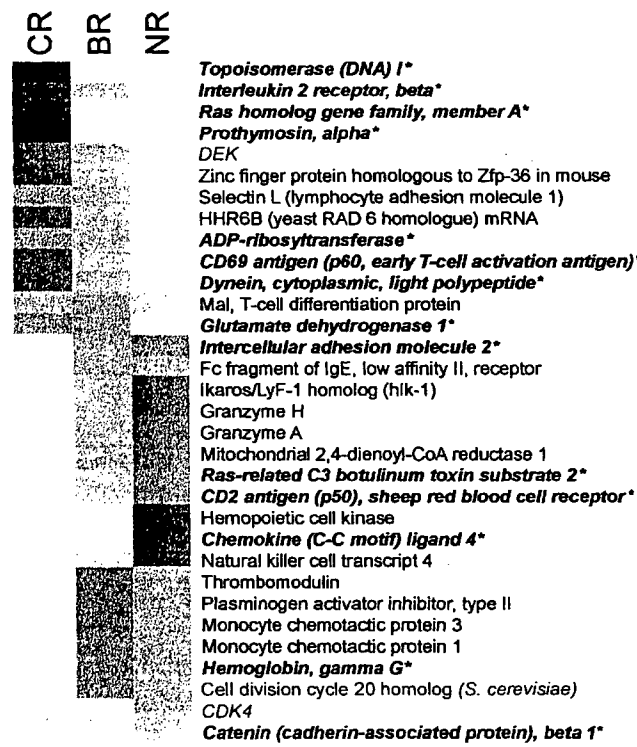

Figure 3. Thirty-two genes screened for gene-expression data before interferon (IFN) therapy by projective adaptive resonance theory. Red indicates up-regulated genes, and blue indicates down-regulated genes. Asterisks indicate genes that are included in table 4. BR, biochemical responder; CR, complete responder; NR, nonresponder.

Table 4. Ten gene combinations selected by the SWEEP operator method for construction of chronic hepatitis C class prediction at the start of interferon (IFN) therapy.

Combination	Input	Gene name	GenBank accession no.	Accuracy, %	
				Training	Test
1	1	***CD2 antigen (p50), sheep red blood cell receptor***[a]	NM_001767	21.2	14.1
	2	Glutamate dehydrogenase 1	NM_005271	72.4	46.2
	3	Dynein, cytoplasmic, light polypeptide	NM_003746	55.8	49.4
2	1	Ras-related C3 botulinum toxin substrate 2	NM_002872	34.6	20.5
	2	Glutamate dehydrogenase 1	NM_005271	81.4	68.6
	3	***Interleukin 2 receptor β***[a]	NM_000878	53.2	43.6
3	1	***Hemoglobin γG***[a]	NM_000184	19.9	16.7
	2	Ras-related C3 botulinum toxin substrate 2	NM_002872	64.7	36.6
	3	Dynein, cytoplasmic, light polypeptide	NM_003746	62.2	58.3
4	1	Intercellular adhesion molecule 2	NM_000873	28.9	26.3
	2	Ras homolog gene family member A	NM_001664	41.7	25.7
	3	Prothymosin α	NM_002823	66.0	47.4
5	1	Topoisomerase (DNA) I	NM_003286	53.9	46.2
	2	Catenin (cadherin-associated protein) β1 (88 kDa)	NM_001904	66.0	57.1
	3	Ras-related C3 botulinum toxin substrate 2	NM_002872	91.0	89.1
6	1	Catenin (cadherin-associated protein) β1 (88 kDa)	NM_001904	44.9	41.0
	2	Topoisomerase (DNA) I	NM_003286	66.0	57.1
	3	Ras-related C3 botulinum toxin substrate 2	NM_002872	91.0	89.1
7	1	Catenin (cadherin-associated protein) β1 (88 kDa)	NM_001904	35.3	31.4
	2	***Interleukin 2 receptor β***[a]	NM_000878	47.4	43.6
	3	ADP-ribosyltransferase (NAD+; poly [ADP-ribose] polymerase)	NM_001618	62.2	60.9
8	1	Chemokine (C-C motif) ligand 4	NM_002984	44.9	41.0
	2	***Interleukin 2 receptor β***[a]	NM_000878	37.8	29.5
	3	Topoisomerase (DNA) I	NM_003286	44.9	34.6
9	1	***Interleukin 2 receptor β***[a]	NM_000878	30.8	30.8
	2	Catenin (cadherin-associated protein) β1 (88 kDa)	NM_001904	47.4	43.6
	3	ADP-ribosyltransferase (NAD+; poly [ADP-ribose] polymerase)	NM_001618	62.2	60.9
10	1	CD69 antigen (p60, early T cell–activation antigen)	NM_001781	42.3	32.1
	2	Prothymosin α	NM_002823	33.3	24.4
	3	Glutamate dehydrogenase 1	NM_005271	39.1	31.4

[a] Genes that present similar expression patterns during IFN and ribavirin combination therapy.

gene-expression profiles of patients with CH-C with those of healthy volunteers. For all 1305 genes, the results of hierarchical clustering analysis, a nonsupervised learning method, confirmed that the gene-expression profiles of PBMCs from the 6 healthy volunteers clearly differed when compared with those of the 13 patients with CH-C (group A) before IFN therapy (figure 1*A*). When the 2 groups were compared by support vector machine, a supervised learning method (BRB-ArrayTools), a total of 48 predictor genes were identified with a significance level of $P < .002$, and it was possible to differentiate the 2 groups with 100% accuracy. Gene parameters (ratio, *T* value, *P* value, description, GenBank accession no., and annotation) are summarized in table 2.

A GO comparison tool (BRB-ArrayTools) identifies more genes that are differentially expressed and are coordinately regulated among predefined clinical groups than expected by chance, thus enabling the finding of biologically related genes to reinforce one another. GO comparison of gene expression between the patients with CH-C and the healthy volunteers revealed significant differences in the Janus kinase signal transducer and activation of transcription (JAK-STAT) cascade, humoral immune response, and G protein–coupled receptor protein signaling pathway ($P < .005$) (table 3). One-way clustering analyses of representative differentially expressed genes are shown in figure 1*B*. These genes were generally activated in PBMCs from patients with CH-C; however, genes such as *CCR2*, monocyte chemoattractant protein 1 receptor, and *IL7R* were significantly down-regulated. The reason for this is not known, but it may reflect infiltration of PBMCs into the liver. The top 20 differentially expressed genes were selected, and gene-expression profiling of these genes in liver-infiltrating lymphocytes was performed (figure 1*C*). Most of the gene-

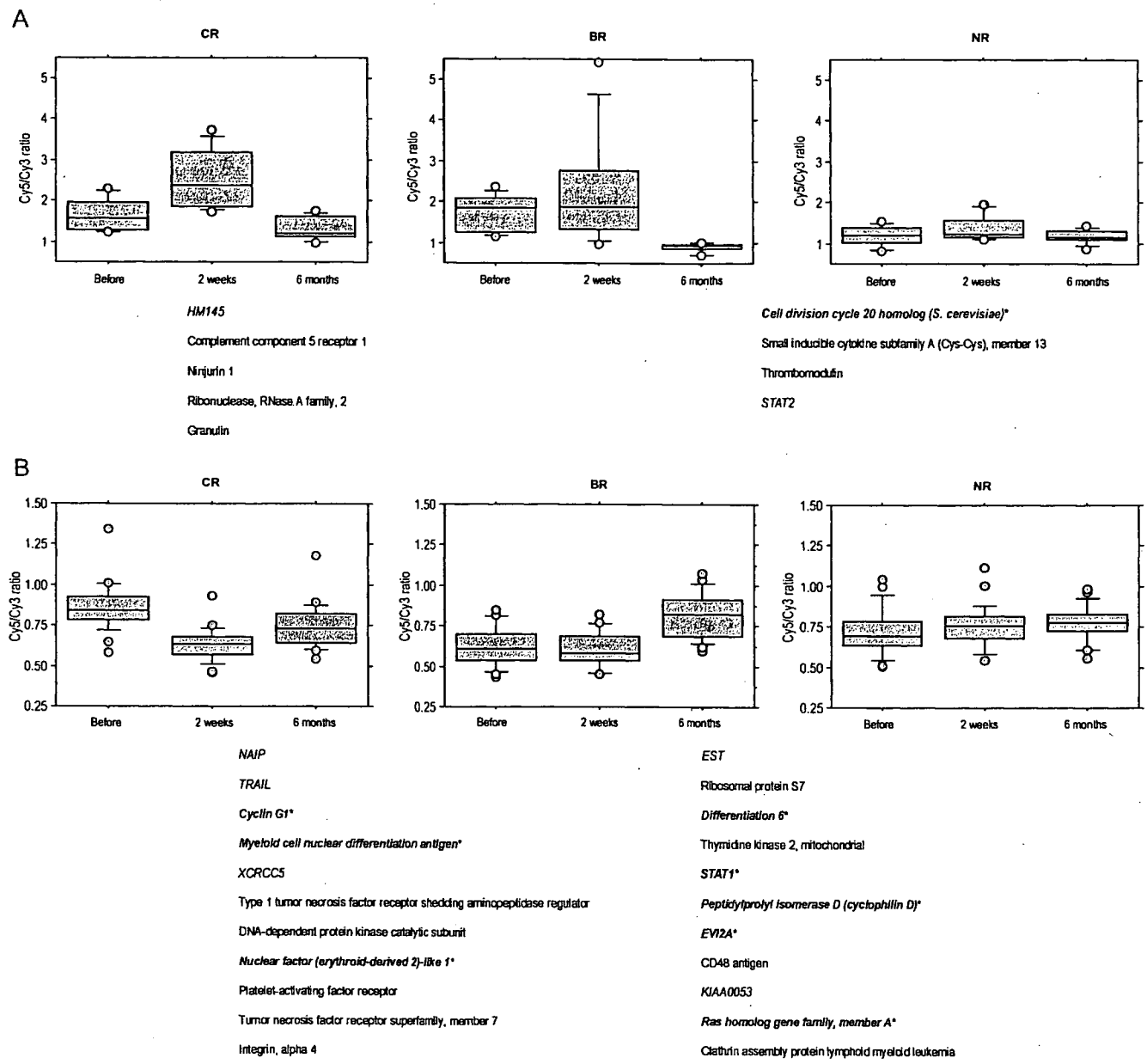

Figure 4. Gene-expression patterns. By use of projective adaptive resonance theory, 86 genes with changes in gene expression before and 2 weeks after the start of interferon (IFN) therapy were selected. For the complete responder (CR) group, changes in the expression of the 86 genes due to IFN therapy were classified into the following 5 patterns, on the basis of self-organizing maps (GeneCluster): up-regulated at 2 weeks after the start of IFN therapy and then down-regulated after the end of IFN therapy *(A)*; down-regulated at 2 weeks after the start of IFN therapy and then up-regulated after the end of IFN therapy *(B)*; up-regulated at 2 weeks after the start of IFN therapy and also up-regulated after the end of IFN therapy *(C)*; up-regulated at 2 weeks after the start of IFN therapy and then returned to normal after the end of IFN therapy *(D)*; and down-regulated at 2 weeks after the start of IFN therapy and also down-regulated after the end of IFN therapy *(E)*. Representative genes are listed under each pattern. Asterisks indicate genes that are included in table 5.

expression ratios for liver-infiltrating lymphocytes showed >1-fold increases compared with hepatocytes, thus indicating that most genes were preferentially expressed in lymphocytes. Interestingly, the genes with increased expression in liver-infiltrating lymphocytes tended to be expressed at lower levels in PBMCs (figure 1*C*).

Serial changes in the differentially expressed genes listed in table 2 during IFN treatment are shown in figure 2*A*. In the

C

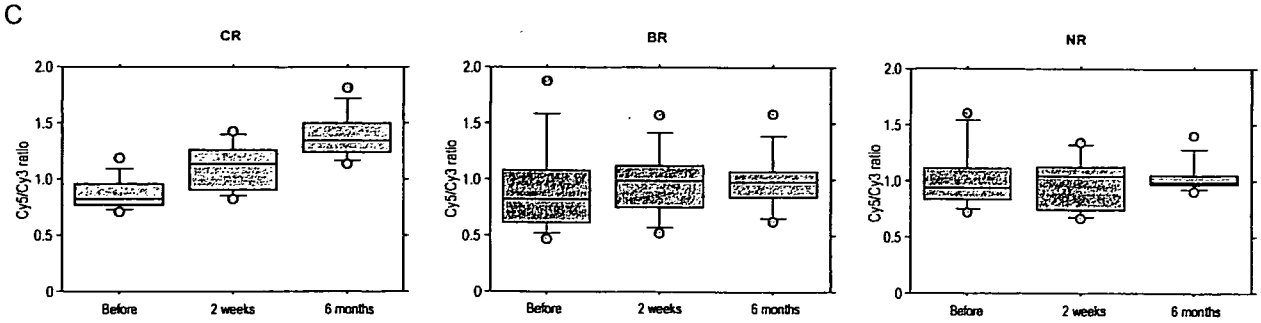

Serine (or cysteine) proteinase inhibitor, clade A*	Bruton agammaglobulinemia tyrosine kinase
Ribosomal protein S27 (metallopanstimulin 1)	*LITAF*
Eukaryotic translation elongation factor 2	Hemopoietic cell kinase
Epidermal growth factor receptor	*GZMA*
Hemopoietic cell kinase	

D

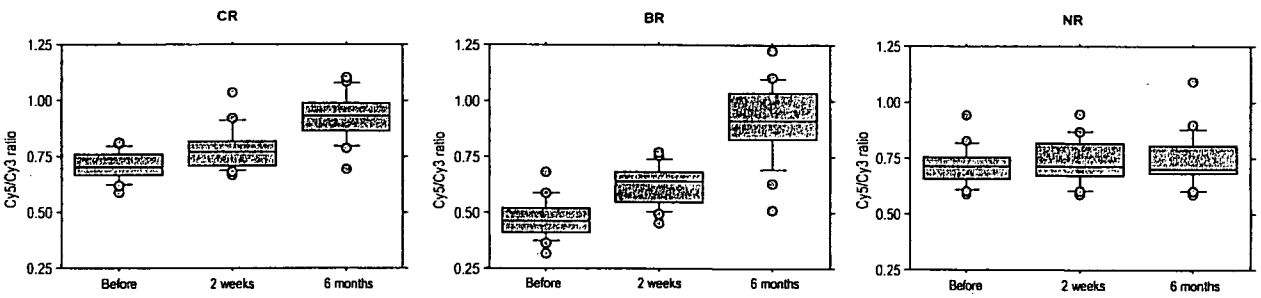

Interleukin 2 receptor beta chain	***ADP-ribosyltransferase****	Semaphorin (CD100)
ICE	Interleukin enhancer binding factor 1	Mitochondrial 2,4-dienoyl-CoA reductase
Ribosomal protein S16	CD3D antigen, delta polypeptid	***Ras-related C3 botulinum toxin substrate 2****
Glutamate dehydrogenase 1	Fc fragment of IgE, low affinity II, receptor	*E2L1*
Small nuclear ribonucleoprotein polypeptide N	Selectin L (lymphocyte adhesion molecule 1)	Citrate synthase
Mutant lymphocyte-specific protein tyrosine kinase	Ikaros/LyF-1 homolog (hlk-1)	*ERP72*

E

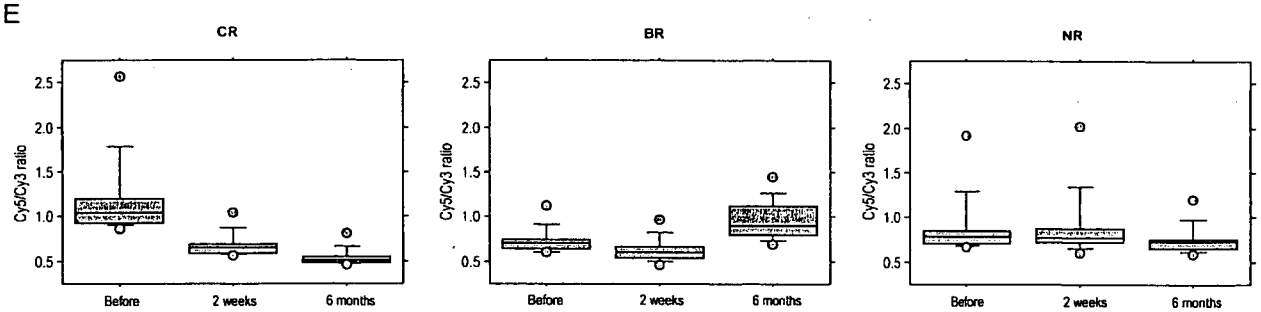

Baculoviral IAP repeat–containing 2*	Rho-associated, coiled-coil containing protein kinase 1
MIHC*	***Apoptosis inhibitor 1****
NRAS-related gene	Uracil-DNA glycosylase
Reticulocalbin 2, EF-hand calcium binding domain	Damage-specific DNA binding protein 1 (127kD)
ERCC5*	CD69 antigen (p60, early T-cell activation antigen)
Integrin, beta 1	

Figure 4. *(Continued.)*

Table 5. Ten gene combinations selected by the SWEEP operator method for the construction of chronic hepatitis C class prediction 2 weeks after the start of interferon (IFN) therapy.

Combination	Input	Gene name	GenBank accession no.	Accuracy, %	
				Training	Test
1	1	*ERCC5*	NM_000123	55.3	45.5
	2	Serine (or cysteine) proteinase inhibitor clade A member 1	NM_000295	85.6	54.5
	3	Ras homolog gene family member A	NM_001664	80.3	70.5
2	1	Baculoviral IAP repeat–containing 2	NM_001166	47.7	41.7
	2	Serine (or cysteine) proteinase inhibitor clade A member 1	NM_000295	80.3	53.8
	3	Ras homolog gene family member A	NM_001664	80.3	70.5
3	1	Cyclin G1	NM_004060	36.6	44.0
	2	Ras-related C3 botulinum toxin substrate 2	NM_002872	79.6	61.4
	3	*EST*		70.5	56.8
4	1	Ecotropic viral integration site 2A	NM_001003927	41.7	25.8
	2	Peptidylprolyl isomerase D (cyclophilin D)	NM_005038	60.6	46.2
	3	Cyclin G1	NM_004060	77.3	67.4
5	1	***Myeloid cell nuclear differentiation antigen***[a]	NM_002432	55.3	25.8
	2	Cyclin G1	NM_004060	85.6	64.4
	3	ADP-ribosyltransferase (NAD+; poly [ADP-ribose] polymerase)	NM_001618	80.3	87.1
6	1	Integrin β1	NM_033666	47.7	19.7
	2	Cyclin G1	NM_004060	80.3	62.9
	3	***STAT1***[a]	NM_139266	80.3	68.2
7	1	Differentiation 6 (septin 2)	NM_004404	28.8	25.8
	2	Cyclin G1	NM_004060	75.0	64.4
	3	Cell division cycle 20 homolog *(S. cerevisiae)*	NM_001255	90.2	87.9
8	1	*MIHC*	NM_001165	28.8	25.0
	2	Cyclin G1	NM_004060	75.0	64.4
	3	Cell division cycle 20 homolog *(S. cerevisiae)*	NM_001255	90.2	87.9
9	1	Apoptosis inhibitor 1 (baculoviral IAP repeat–containing 3)	NM_001165	28.8	25.0
	2	Cyclin G1	NM_004060	75.0	64.4
	3	Cell division cycle 20 homolog *(S. cerevisiae)*	NM_001255	90.2	87.9
10	1	Nuclear factor (erythroid-derived 2)–like 1	NM_003204	25.0	25.8
	2	Cyclin G1	NM_004060	75.0	63.6
	3	ADP-ribosyltransferase (NAD+; poly [ADP-ribose] polymerase)	NM_001618	88.6	81.8

[a] Genes that present similar expression patterns during IFN and ribavirin combination therapy.

CR group, the expression profiles of genes that were either up- or down-regulated before IFN therapy were similar to those of healthy volunteers 6 months after the end of IFN therapy (figure 2*A*, CR group). On the other hand, in the NR group, expression of genes that were either up- or down-regulated before IFN therapy tended to remain up- or down-regulated 6 months after the end of IFN therapy (figure 2*A*, NR group). This suggests that the changes in gene-expression profiles of patients with CH-C before IFN therapy reflect the state of HCV infection.

We performed real-time PCR to corroborate the microarray data. Real-time PCR revealed that *CD69* was up-regulated in patients with CH-C and that *CCR2* and *IL7R* were down-regulated in patients with CH-C (figure 2*B* and table 2).

Relationship between PBMC gene-expression profiles and IFN response. We then analyzed the relationship between PBMC gene-expression profiles before the start of IFN therapy and IFN response. Because the regimen of IFN treatment was different in group A and group B patients, we first focused on group A patients (table 1). In hierarchical clustering analysis using all genes before IFN therapy, no clustering was seen in the CR, BR, or NR groups. Conventional supervised learning methods, such as support vector machine and nearest neighbor (BRB-ArrayTools), could not discriminate between the CR, BR, and NR groups. Therefore, we applied the FNN-SWEEP method to predict the outcome of IFN therapy. Before FNN-

Table 6. Comparison of interferon (IFN)–stimulated gene (ISG) expression induced by IFN.

The table is available in its entirety in the online edition of the *Journal of Infectious Diseases*.

SWEEP analysis, nonspecific genes or genes with errors were eliminated by the PART method. The 32 genes screened by PART are shown in figure 3. Topoisomerase (DNA) I *(TOP1)* and interleukin 2 receptor β *(IL2RB)* were up-regulated in the CR group, hemoglobin γG *(HBG2)* and monocyte chemotactic protein were up-regulated in the BR group, and chemokine (C-C motif) ligand 4 and ras-related C3 botulinum toxin substrate 2 *(RAC2)* were up-regulated in the NR group. Genes selected by PART were subjected to the FNN-SWEEP method to construct a class prediction model. Consequently, we selected 10 gene combinations by the SWEEP operator method for CH-C class prediction before the start of IFN therapy (table 4). The most effective gene combination for the prediction of an IFN response was *TOP1;* catenin (cadherin-associated protein) β1 (88 kDa); and *RAC2.* The accuracy of the training and test sets were high, at 91.0% and 89.1%, respectively.

Changes in gene-expression profiles over the course of IFN therapy. We next focused on the changes in gene-expression profiles over the course of IFN therapy and their relationship with IFN response. Using PART, 86 genes with changes in expression between before and 2 weeks after the start of IFN therapy were selected. To investigate the relationship between the 86 genes with changes due to IFN therapy and the efficacy of IFN therapy, changes in the expression of the 86 genes were determined for the CR group. On the basis of self-organizing maps, changes in gene expression in the CR group were classified into the following 5 patterns (figure 4): pattern A, up-regulated 2 weeks after the start of IFN therapy and then down-regulated after the end of IFN therapy; pattern B, down-regulated 2 weeks after the start of IFN therapy and then up-regulated after the end of IFN therapy; pattern C, up-regulated 2 weeks after the start of IFN therapy and also up-regulated after the end of IFN therapy; pattern D, up-regulated at 2 weeks after the start of IFN therapy and then returned to normal after the end of IFN therapy; and pattern E, down-regulated at 2 weeks after the start of IFN therapy and also down-regulated after the end of IFN therapy. Patterns A and B represent gene groups with temporary changes during IFN therapy, whereas patterns C, D, and E represent gene groups with changes after the end of IFN therapy and are thought to be attributable to viral eradication or normalization of hepatic function. Interestingly, very little change was seen in the patterns for the NR group. Therefore, changes in gene expression are also useful in predicting therapeutic efficacy. From the 86 genes isolated by PART, the SWEEP operator method was used to identify 10 gene combinations, and therapeutic efficacy was predicted according to the FNN-SWEEP method (table 5). The results showed that the accuracy for gene combinations 7, 8, and 9 was high, at 90.2%. LOOCV confirmed the high accuracy (87.9%) of prediction using these gene combinations. These combinations included the following genes that are important for predicting therapeutic efficacy: *CDC20* was classified as belonging to pattern A; cyclin G1 and differentiation 6 were as belonging to pattern B; and *MIHC* and apoptosis inhibitor 1 were as belonging to pattern E (figure 4).

IFN and ribavirin combination therapy. We then investigated the usefulness of the above-mentioned genes in predicting the efficacy of IFN and ribavirin combination therapy. It has been shown that concurrent ribavirin administration improves the rate of CR. In addition, the changes in gene expression during combination therapy are due not only to IFN but also to ribavirin. Thus, the results for monotherapy may not be applicable to combination therapy. However, changes in the expression of several genes—CD2 antigen (p50), *IL2RB, HBG2,* myeloid cell nuclear differentiation antigen *(MNDA),* and *STAT1*—were shown to be extremely useful for distinguishing CR from NR in IFN and ribavirin combination therapy (tables 4 and 5).

DISCUSSION

HCV load, genotype, and fibrosis have been listed as factors that influence the effectiveness of IFN therapy [4, 5], but these factors are not sufficient, and other predictive factors are needed. Unlike liver-biopsy specimens, PBMCs can be easily collected, and collection can be repeated as necessary. We analyzed the gene-expression profiles of PBMCs in patients with CH-C by use of cDNA microarrays under the hypothesis that gene expression in PBMCs is indicative of IFN efficacy and CH-C disease state. In addition, changes in the gene-expression profiles of PBMCs were analyzed during the course of IFN therapy to clarify the relationship between gene-expression profiles of PBMCs and IFN response.

Interestingly, the gene-expression profiles of PBMCs from patients with CH-C and from healthy volunteers were different, and this was confirmed by hierarchical clustering analysis and supervised learning analysis using support vector machine. When patients with CH-C and healthy volunteers were compared, gene expression in the JAK-STAT cascade, humoral immune response, and G protein–coupled receptor protein signaling pathway differed markedly. In most patients with CH-C, expression of these genes is activated, and HCV infection is thought to bring about changes in the gene expression in PBMCs. Several chemokine- and cytokine-related genes, such as *CCR2* and *IL7R,* were down-regulated. Although the reason for this was not clear, expression of these genes in liver-infiltrating lymphocytes was up-regulated. Therefore, the down-regulation of immune-related genes may represent increased levels of liver-infiltrating lymphocytes accompanying hepatitis. Interestingly, when the chronological changes in PBMC gene-expression profiles were analyzed for the CR group, the profiles at 6 months after the end of therapy were similar to those of healthy volunteers. Therefore, the changes in gene-expression

profiles before IFN therapy were due to HCV infection. On the other hand, the gene-expression profiles of the NR group before IFN therapy were similar to those at 6 months after the end of IFN therapy (figure 2*A*).

Unfortunately, it was not possible to differentiate between CR, BR, and NR patients on the basis of gene-expression profiles of PBMCs by use of nonsupervised learning methods, such as hierarchical clustering, before IFN therapy. Therefore, we used FNN theory for CH-C class prediction. The most attractive feature of FNN is that causality between input and output variables can be described very accurately as explicit if-then roles obtained from the constructed model. For the purpose of analyzing numerous genes in a short time, FNN combined with the SWEEP operator method was developed (FNN-SWEEP method) and has been shown to be a precise, simple tool for predicting patient survival on the basis of microarray data [28, 29]. In addition, by first filtering genes by use of PART, the accuracy of the FNN-SWEEP method was further increased [30]. In the present study, a total of 32 genes were identified by PART on the basis of genetic changes before therapy, and, in the CR group, expression of genes such as *TOP1*, *IL2RB*, prothymosin α *(PTMA)*, and ADP-ribosyltransferase was up-regulated, thus indicating active cellular proliferation. In the NR group, the expression of genes indicating activated cytotoxic T cells—such as granzyme, CD2 antigen, *RAC2*, and natural killer cell transcript 4—was up-regulated. Because these genes were up-regulated by IFN therapy in the CR group, they were thought to be up-regulated before therapy in the NR group. Lempicki et al. reported elevated expression of endogenous IFN/innate immune response genes in PBMCs from NR patients coinfected with HCV and HIV [31]. This suggests that, in many NR patients, few immune effector cells are active or that these effector cells cannot infiltrate the liver and remain in the peripheral blood.

To further investigate the above-mentioned points, changes in the gene-expression profiles of PBMCs were determined during the course of IFN therapy. On the basis of expression profiles before and 2 weeks after the start of IFN therapy, 86 genes were selected. These genes did not include as many IFN-α–stimulated genes as were noted in liver [25–27] (table 6), but they included valuable immune regulatory genes.

On the basis of self-organizing maps, changes in gene expression in the CR group were then classified into 5 patterns (figure 4). These gene groups represent genes with temporary changes due to IFN therapy and those with changes after the end of IFN therapy. Gene groups with changes after the end of IFN therapy are thought to be involved in viral eradication or the normalization of hepatic function. Interestingly, little change was seen in any of the patterns in the NR group. In efficacy prediction by the FNN-SWEEP method, the accuracy for the gene combinations 7, 8, and 9 was high, at 90.2%, thus suggesting that changes in gene expression 2 weeks after the start of IFN therapy are also useful in predicting therapeutic efficacy.

We also investigated whether these genes are useful in predicting the efficacy of IFN and ribavirin combination therapy. Changes in gene expression during combination therapy were due not only to IFN but also to ribavirin, and the results for monotherapy could not simply be applied to combination therapy. However, changes in the expression of several genes—CD2 antigen (p50), *IL2RB*, *HBG2*, *MNDA*, and *STAT1*—were shown to be extremely useful for distinguishing CR from NR in IFN and ribavirin combination therapy.

Unfortunately, because the number of subjects in the present study was small, the genes that were identified as predictors for IFN monotherapy were not necessarily predictors for IFN and ribavirin combination therapy. However, the present study was the first to show that responses to IFN therapy could be predicted on the basis of changes in gene expression by PBMCs, and further investigations in greater numbers of patients are required.

Acknowledgments

We thank Prof. Kenichi Kobayashi, for helpful discussion and advice. We also thank A. Nakano, M. Ueda, and J. Hara, for their valuable technical assistance.

References

1. McHutchison JG, Gordon SC, Schiff ER, et al. Interferon alfa-2b alone or in combination with ribavirin as initial treatment for chronic hepatitis C. Hepatitis Interventional Therapy Group. N Engl J Med **1998**; 339:1485–92.
2. Davis GL, Esteban-Mur R, Rustgi V, et al. Interferon alfa-2b alone or in combination with ribavirin for the treatment of relapse of chronic hepatitis C. International Hepatitis Interventional Therapy Group. N Engl J Med **1998**; 339:1493–99.
3. Poynard T, Marcellin P, Lee SS, et al. Randomised trial of interferon alpha2b plus ribavirin for 48 weeks or for 24 weeks versus interferon alpha2b plus placebo for 48 weeks for treatment of chronic infection with hepatitis C virus. International Hepatitis Interventional Therapy Group. Lancet **1998**; 352:1426–32.
4. Martinot-Peignoux M, Marcellin P, Pouteau M, et al. Pretreatment serum hepatitis C virus RNA levels and hepatitis C virus genotype are the main and independent prognostic factors of sustained response to interferon alfa therapy in chronic hepatitis C. Hepatology **1995**; 22: 1050–6.
5. Tsubota A, Chayama K, Ikeda K, et al. Factors predictive of response to interferon-alpha therapy in hepatitis C virus infection. Hepatology **1994**; 19:1088–94.
6. Mizukoshi E, Kaneko S, Yanagi M, et al. Expression of interferon alpha/beta receptor in the liver of chronic hepatitis C patients. J Med Virol **1998**; 56:217–23.
7. Ortaldo JR, Mantovani A, Hobbs D, Rubinstein M, Pestka S, Herberman RB. Effects of several species of human leukocyte interferon on cytotoxic activity of NK cells and monocytes. Int J Cancer **1983**; 31: 285–9.
8. Tsubouchi E, Akbar SM, Horiike N, Onji M. Infection and dysfunction

of circulating blood dendritic cells and their subsets in chronic hepatitis C virus infection. J Gastroenterol 2004; 39:754–62.
9. Popov S, Chenine AL, Gruber A, Li PL, Ruprecht RM. Long-term productive human immunodeficiency virus infection of CD1a-sorted myeloid dendritic cells. J Virol 2005; 79:602–8.
10. Schena M, Shalon D, Davis RW, Brown PO. Quantitative monitoring of gene expression patterns with a complementary DNA microarray. Science 1995; 270:467–70.
11. Schena M, Shalon D, Heller R, Chai A, Brown PO, Davis RW. Parallel human genome analysis: microarray-based expression monitoring of 1000 genes. Proc Natl Acad Sci USA 1996; 93:10614–9.
12. DeRisi J, Penland L, Brown PO, et al. Use of a cDNA microarray to analyse gene expression patterns in human cancer. Nat Genet 1996; 14:457–60.
13. Khan J, Simon R, Bittner M, et al. Gene expression profiling of alveolar rhabdomyosarcoma with cDNA microarrays. Cancer Res 1998; 58: 5009–13.
14. Iyer VR, Eisen MB, Ross DT, et al. The transcriptional program in the response of human fibroblasts to serum. Science 1999; 283:83–7.
15. Heller RA, Schena M, Chai A, et al. Discovery and analysis of inflammatory disease-related genes using cDNA microarrays. Proc Natl Acad Sci USA 1997; 94:2150–5.
16. Alizadeh AA, Eisen MB, Davis RE, et al. Distinct types of diffuse large B-cell lymphoma identified by gene expression profiling. Nature 2000; 403:503–11.
17. Desmet VJ, Gerber M, Hoofnagle JH, Manns M, Scheuer PJ. Classification of chronic hepatitis: diagnosis, grading and staging. Hepatology 1994; 19:1513–20.
18. Tanaka T, Tsukiyama-Kohara K, Yamaguchi K, et al. Significance of specific antibody assay for genotyping of hepatitis C virus. Hepatology 1994; 19:1347–53.
19. Kawai HF, Kaneko S, Honda M, Shirota Y, Kobayashi K. Alpha-fetoprotein-producing hepatoma cell lines share common expression profiles of genes in various categories demonstrated by cDNA microarray analysis. Hepatology 2001; 33:676–91.
20. Honda M, Kaneko S, Kawai H, Shirota Y, Kobayashi K. Differential gene expression between chronic hepatitis B and C hepatic lesion. Gastroenterology 2001; 120:955–66.
21. Shirota Y, Kaneko S, Honda M, Kawai HF, Kobayashi K. Identification of differentially expressed genes in hepatocellular carcinoma with cDNA microarrays. Hepatology 2001; 33:832–40.
22. Honda M, Shimazaki T, Kaneko S. La protein is a potent regulator of replication of hepatitis C virus in patients with chronic hepatitis C through internal ribosomal entry site-directed translation. Gastroenterology 2005; 128:449–62.
23. Kawaguchi K, Honda M, Yamashita T, Shirota Y, Kaneko S. Differential gene alteration among hepatoma cell lines demonstrated by cDNA microarray-based comparative genomic hybridization. Biochem Biophys Res Commun 2005; 329:370–80.
24. Honda M, Kawai H, Shirota Y, Yamashita T, Kaneko S. Differential gene expression profiles in stage I primary biliary cirrhosis. Am J Gastroenterol 2005; 100:2019–30.
25. Honda M, Yamashita T, Ueda T, Takatori H, Nishino R, Kaneko S. Different signaling pathways in the livers of patients with chronic hepatitis B or chronic hepatitis C. Hepatology 2006; 44:1122–38.
26. Smith MW, Walters KA, Korth MJ, et al. Gene expression patterns that correlate with hepatitis C and early progression to fibrosis in liver transplant recipients. Gastroenterology 2006; 130:179–87.
27. Bigger CB, Guerra B, Brasky KM, et al. Intrahepatic gene expression during chronic hepatitis C virus infection in chimpanzees. J Virol 2004; 78:13779–92.
28. Ando T, Suguro M, Kobayashi T, Seto M, Honda H. Selection of casual gene sets for lymphoma prognostication from expression profiling and construction of prognostic fuzzy neural network models. J Biosci Bioeng 2003; 96:161–7.
29. Ando T, Suguro M, Kobayashi T, Seto M, Honda H. Multiple fuzzy neural network system for outcome prediction and classification of 220 lymphoma patients on the basis of molecular profiling. Cancer Sci 2003; 94:906–13.
30. Takahashi H, Kobayashi T, Honda H. Construction of robust prognostic predictors by using projective adaptive resonance theory as a gene filtering method. Bioinformatics 2005; 21:179–86.
31. Lempicki RA, Polis MA, Yang J, et al. Gene expression profiles in hepatitis C virus (HCV) and HIV coinfection: class prediction analyses before treatment predict the outcome of anti-HCV therapy among HIV-coinfected persons. J Infect Dis 2006; 193:1172–7.

Natural killer cell and hepatic cell interaction via NKG2A leads to dendritic cell-mediated induction of CD4$^+$ CD25$^+$ T cells with PD-1-dependent regulatory activities

Masahisa Jinushi, Tetsuo Takehara, Tomohide Tatsumi, Shinjiro Yamaguchi, Ryotaro Sakamori, Naoki Hiramatsu, Tatsuya Kanto, Kazuyoshi Ohkawa and Norio Hayashi

Department of Gastroenterology and Hepatology, Osaka University Graduate School of Medicine, Osaka, Japan

doi:10.1111/j.1365-2567.2006.02479.x
Received 24 June 2006; revised 24 August 2006; accepted 24 August 2006.
Correspondence: Norio Hayashi MD, Department of Gastroenterology and Hepatology, Osaka University Graduate School of Medicine, 2–2 Yamada-oka, Suita, Osaka 565-0871, Japan.
Email: hayashin@gh.med.osaka-u.ac.jp
Senior author: Tetsuo Takehara, email: takehara@gh.med.osaka-u.ac.jp

Summary

Natural killer (NK) cells have the ability to control dendritic cell (DC)-mediated T cell responses. However, the precise mechanisms by which NK receptor-mediated regulation of NK cells determines the magnitude and direction of DC-mediated T cell responses remain unclear. In the present study, we applied an *in vitro* co-culture system to examine the impact of NK cells cultured with hepatic cells on DC induction of regulatory T cells. We found that interaction of NK cells and non-transformed hepatocytes (which express HLA-E) via the NKG2A inhibitory receptor resulted in priming of DCs to induce CD4$^+$ CD25$^+$ T cells with regulatory properties. NKG2A triggering led to characteristic changes of the cytokine milieu of co-cultured cells; an increase in the transforming growth factor (TGF)-β involved in the generation of this specific type of DC, and a decrease in the tumour necrosis factor-α capable of antagonizing the effect of TGF-β. The regulatory cells induced by NK cell-primed DCs exert their suppressive actions through a negative costimulator programmed death-1 (PD-1) mediated pathway, which differs from freshly isolated CD4$^+$ CD25$^+$ T cells. These findings provide new insight into the role of NK receptor signals in the DC-mediated induction of regulatory T cells.

Keywords: NK receptor; regulatory T cell; HLA-E; liver; HCV

Introduction

CD4$^+$ CD25$^+$ regulatory T (Treg) cells have been identified as the main suppressors of immune responses.[1–5] Although the mechanisms by which CD4$^+$ CD25$^+$ Treg cells exert their suppressive actions have not been fully elucidated, negative costimulatory signals via cytotoxic T lymphocyte antigen-4 (CTLA-4) or inducible costimulator (ICOS)-mediated signals, have been suggested to play a key role in the activation of CD4$^+$ CD25$^+$ Treg cells.[6,7] Programmed death-1 (PD-1), another molecule identified as a negative costimulatory receptor, has also serves as a negative regulator for effector immune responses.[8] Recent reports have demonstrated that PD-1 is expressed in CD4$^+$ CD25$^+$ Treg cells, suggesting its potential roles in the regulation of T cell tolerance.[9] However, the precise roles of PD-1 in CD4$^+$ CD25$^+$ Treg cell functions remain elusive.

The mechanisms by which CD4$^+$ CD25$^+$ Treg cells are generated have been extensively investigated. Dendritic cells (DCs), the sentinels between innate and adaptive immunity, have recently emerged as candidate cells involved in the differentiation and/or activation of CD4$^+$ CD25$^+$ Treg cells.[10] Various kinds of factors have been identified as involved in DC induction of CD4$^+$ CD25$^+$ Treg cells. Mouse immature DC promotes the differentiation of CD4$^+$ CD25$^+$ Treg cells through the DEC 205-mediated targeting of self-antigen in the steady state.[10,11] The immune regulatory cytokines interleukin (IL)-10/transforming growth factor (TGF)-β have also been reported to play important roles in DC generation and activation of CD4$^+$ CD25$^+$ Treg cells.[12–14]

Abbreviations: CTLA-4, cytotoxic T lymphocyte antigen-4; DC, dendritic cell; ELISA, enzyme-linked immunosorbent assay; GITR, glucocorticoid-induced TNF receptor; HCV, hepatitis C virus; HLA, human leucocyte antigen; NH, human non-transformed hepatocyte; NK, natural killer; PD-1, programmed death-1; PDL-1, programmed death ligand 1; PBMC, peripheral blood mononuclear cell; Treg, regulatory T.

Several lines of evidence have revealed that natural killer (NK) cell-mediated innate immunity regulates DC functions to determine the direction and magnitude of adaptive T cell immunity.[15–18] It has also been established that NK cell function is regulated by positive and negative signals through their receptor and ligand interactions.[19] We previously reported that, upon exposure to non-transformed hepatocytes (NHs), IL-2-primed NK cells negatively regulated DC functions, which appeared to be dependent on NKG2A inhibitory signals during co-culture of NK cells and NHs. Immunosuppressive cytokines such as IL-10 and TGF-β, but not direct NK–DC contact, were responsible for this action.[20] However, it remains unclear whether these NK/hepatocyte co-cultures can also influence the induction as well as activation of $CD4^+$ $CD25^+$ Treg cells.

In the present study, we investigated whether DCs stimulated with the co-culture supernatant of IL-2-prestimulated NK cells and NHs can modulate Treg cell functions. We found that TGF-β produced from NK cell/hepatocyte co-culture via NKG2A activation is responsible for modulating DCs to induce and maintain regulatory phenotypes and functions of $CD4^+$ $CD25^+$ Treg cells. Furthermore, the generated $CD4^+$ $CD25^+$ Treg cells suppressed T cell activation via interaction between PD-1 and programmed death ligand 1 (PDL-1). These findings represent new evidence that NK receptor-mediated modulation of NK cells may dictate DC-induced adaptive immunity toward an immunogenic or tolerogenic status via induction of Treg cells.

Materials and methods

Antibodies

Anti-NKG2A monoclonal antibody (mAb) (Z199), PC5-labelled CD25 mAb or isotype-matched control IgG1 and IgG2a mAb were purchased from Beckmann-Coulter (Fullerton, CA). Anti-IL-10, anti-TGF-β, anti-CTLA-4, anti-GITR (glucocorticoid-induced TNF receptor) and anti-PD-1 polyclonal Abs were purchased from R & D Systems (Minneapolis, MN) and phycoerythrin (PE)-labelled mAb CTLA-4 from BD Biosciences (San Jose, CA). Anti-HLA-E mAb 3D12 was kindly provided by Dr E. Geraghty (Fred Hutchinson Cancer Research Institute, Seattle, WA) and used as reported previously.[21] Anti-MIC mAb 6D4, anti-ULBP1 mAb 3F1 and anti-ULBP2 mAb DH1 were kindly provided by Drs T. Spies and V. Groh (Fred Hutchinson Cancer Research Institute) and used as reported previously.[22]

Human hepatic cells

Human non-transformed hepatocytes (NHs) derived from mixed heterogeneous donors were purchased from the Applied Cell Biology Research Institute (Kirkland, WA) and cultured in CS-C complete medium according to the manufacturer's instructions.

Isolation of peripheral blood lymphocyte populations

Resting NK cells ($CD56^+$ $CD3^+$), naive $CD4^+$ T cells ($CD45RA^+$ RO^+) or $CD8^+$ T cells were isolated from peripheral blood mononuclear cells (PBMCs) with a positive cell isolation kit according to the manufacturer's protocol (Miltenyi Biotec, Bergisch Gladbach, Germany). $CD4^+$ $CD25^+$ T cells were further separated from naive $CD4^+$ T cells using anti-CD25 microbeads (Miltenyi Biotech). Their purity was >90% by flow cytometry. Informed consent was obtained from all blood donors.

Generation of monocyte-derived DC

Monocytes were isolated by plastic adherence from PBMCs and cultured in RPMI-1640 supplemented with granulocyte–macrophage colony stimulating factor (GM-CSF) (PeproTech, London, UK) and IL-4 (PeproTech). At day 6, they were stimulated with or without the co-culture supernatant of NK cells and hepatic cells. At day 7, non-adherent cells were harvested and used as described below.

Stimulation of DCs by co-culture supernatants of NK cells and hepatic cells

Freshly isolated NK cells were cultured with or without IL-2 for 24 hr. IL-2-prestimulated or non-stimulated NK cells were seeded in 24-well plates and then co-cultured for 24 hr with NHs (1×10^5 cells/well), respectively. Monocyte-derived DCs were cultured for 24 hr with 1 ml of the co-culture supernatant of IL-2-prestimulated NK cells and NHs (NH/IL-2 NK-primed DC). In some experiments, anti-NKG2A mAb (Z199) or isotype-matched control Ab was added during the co-cultures of NK cells and hepatic cells. Z199 mAb was previously confirmed to block the NKG2A-mediated signal.[23] In some experiments, the supernatant of NK/hepatic cell co-cultures was also treated with anti-IL-10 or anti-TGF-β neutralizing Ab and used for DC stimulation for 24 hr. In some experiments, tumour necrosis factor (TNF)-α, TGF-β or both were used for DC stimulation for 24 hr.

Isolation of $CD4^+$ $CD25^+$ T cells

DCs (1×10^5) were stimulated for 24 hr with the supernatant obtained from the co-cultured medium. After washing three times, DCs were cultured with allogeneic $CD4^+$ T cells for 48 hr; $CD4^+$ $CD25^+$ fractions were isolated from DC and $CD4^+$ co-culture and subjected to further analysis. $CD4^+$ $CD25^+$ fractions were also isolated

from PBMCs and cultured with 1 μg/ml plate-bound anti-CD3 mAb (UCHT1; Beckmann-Coulter) for 24 hr to efficiently induce their suppressive properties as described previously.[3] These cells are referred to as natural $CD4^+$ $CD25^+$ T cells.

Flow cytometry

The expression of NK inhibitory ligands (human leucocyte antigen, HLA, class I, HLA-E) was examined on NHs by using w6/32 or 3D12, respectively. MIC, ULBP1 or ULBP2 expression on hepatocytes was also evaluated by mAb 6D4, 3F1 or DH1, respectively. For $CD4^+$ $CD25^+$ T cell staining, the cells were costained with PC5-labelled CD25 mAb with PE-labelled mAb of CTLA-4, GITR or PD-1 polyclonal Ab. The cells were analysed by flow cytometry using a fluorescence-activated cell sorter (FACScan) system, and data analysis was performed using CELLQUEST software.

Measurements of cytokine production in culture supernatant

The culture supernatants of interferon (IFN)-γ, TNF-α, IL-10 and TGF-β were examined using enzyme-linked immunosorbent assay (ELISA) kits according to the manufacturers' instructions (IFN-γ, TNF-α and IL-10, Endogen, Tokyo, Japan; TGF-β, R & D Systems).

Analysis of Foxp3 mRNA expression

Polymerase chain reaction (PCR) analysis was performed to determine Foxp3 mRNA expression of $CD4^+$ T cells using a commercial PCR panel according to the manufacturer's instructions (Gibco BRL, Rockville, MD). The following primers were used: 5′-CCCACTTACAGGCACT CCTC-3′ (forward) and 5′-CTTCTCCTTCTCCAGCAC CA-3′ (reverse).[24] Amplification was carried out for 35 cycles of 20 seconds at 95°, 20 seconds at 58 ° and 30 seconds at 72°. As a control for the integrity of mRNA, primers specific for GAPDH (glyceraldehyde 3-phosphate dehydrogenase) were used as follows: 5′-GCCACCCAGAAGACTGTGGATGGC-3′ (forward) and 5′-CATGTAGGCCATGAGGTCCACCAC-3′ (reverse). The PCR products were analysed by ethidium bromide-stained 1·5% agarose gel electrophoresis.

Analysis of $CD4^+$ $CD25^+$ T cell suppressor functions

DCs (5×10^4/well) were cultured with allogeneic $CD4^+$ T cells (5×10^5/well) for 48 hr, after which $CD4^+$ $CD25^+$ T cells were isolated from the co-cultured cells. $CD4^+$ $CD25^-$ T cells were freshly isolated from the same donors and activated with 1 μg/ml plate-bound anti-CD3 mAb in the presence or absence of autologous $CD4^+$ $CD25^+$ T cells for 48 hr. The ability of $CD4^+$ $CD25^+$ T cells to suppress proliferation and IFN-γ production of activated $CD4^+$ $CD25^-$ T cells was determined by [^{3}H]thymidine incorporation and ELISA assay, respectively. To further examine the mechanisms of $CD4^+$ $CD25^+$ T cell suppressive actions, neutralizing Ab of IL-10 or TGF-β, anti-CTLA-4, anti-GITR or anti-PD-1 was added at the beginning of $CD4^+$ $CD25^+$ T cell and $CD4^+$ $CD25^-$ T cell co-cultures.

Statistical analysis

Comparisons between groups were analysed by *t*-test with Welch's correction or ANOVA for experiments with more than two subgroups. Differences were considered significant when the *P*-value was < 0.05.

Results

IL-2-primed NK cells upon exposure to NH-modulated DCs on the induction of regulatory $CD4^+$ $CD25^+$ T cells

Natural $CD4^+$ $CD25^+$ T cells from human peripheral blood lymphocytes (PBLs) expressed CTLA-4 and GITR, both of which have been identified as regulatory markers,[6,25] but did not express PD-1 (Fig. 1a). To examine whether DCs can modulate the expression of these regulatory markers on $CD4^+$ $CD25^+$ T cells, we stimulated monocyte-derived DCs for 24 hr, either by the culture supernatant of IL-2-stimulated NK cells (IL-2 NK) or by the co-culture supernatant of NH/IL-2 NK. After washing, the resulting DCs were cultured for 48 hr with $CD4^+$ T cells isolated from allogeneic donors. $CD4^+$ $CD25^+$ T cells were isolated from the DC and $CD4^+$ T cell co-culture and subjected to analysis for regulatory markers. The expression levels of CTLA-4 and GITR decreased on $CD4^+$ $CD25^+$ T cells after stimulation of IL-2 NK-primed DCs (Fig. 1b). By contrast, $CD4^+$ $CD25^+$ T cells stimulated with NH/IL-2 NK-primed DCs remained positive for CTLA-4 and GITR on their surface. Of note is the finding that PD-1 was induced on these cells, showing their phenotypic properties to differ from natural $CD4^+$ $CD25^+$ T cells (Fig. 1b, c). The induction of PD-1 on $CD4^+$ $CD25^+$ T cells was further confirmed when IL-2NK/NH-primed DCs from different donors were used as stimulators (Fig. 1d). The supernatant of NH without NK cells had little effect on phenotypic changes of $CD4^+$ $CD25^+$ T cells by DCs (data not shown).

The forkhead transcription factor Foxp3 has been recently identified as a master gene for defining Treg cells.[26] We therefore performed reverse transcription-PCR (RT-PCR) analysis of $CD4^+$ T cells to evaluate the mRNA expression of Foxp3. Foxp3 expression was detected in natural $CD4^+$ $CD25^+$ T cells. When $CD4^+$ T cells were

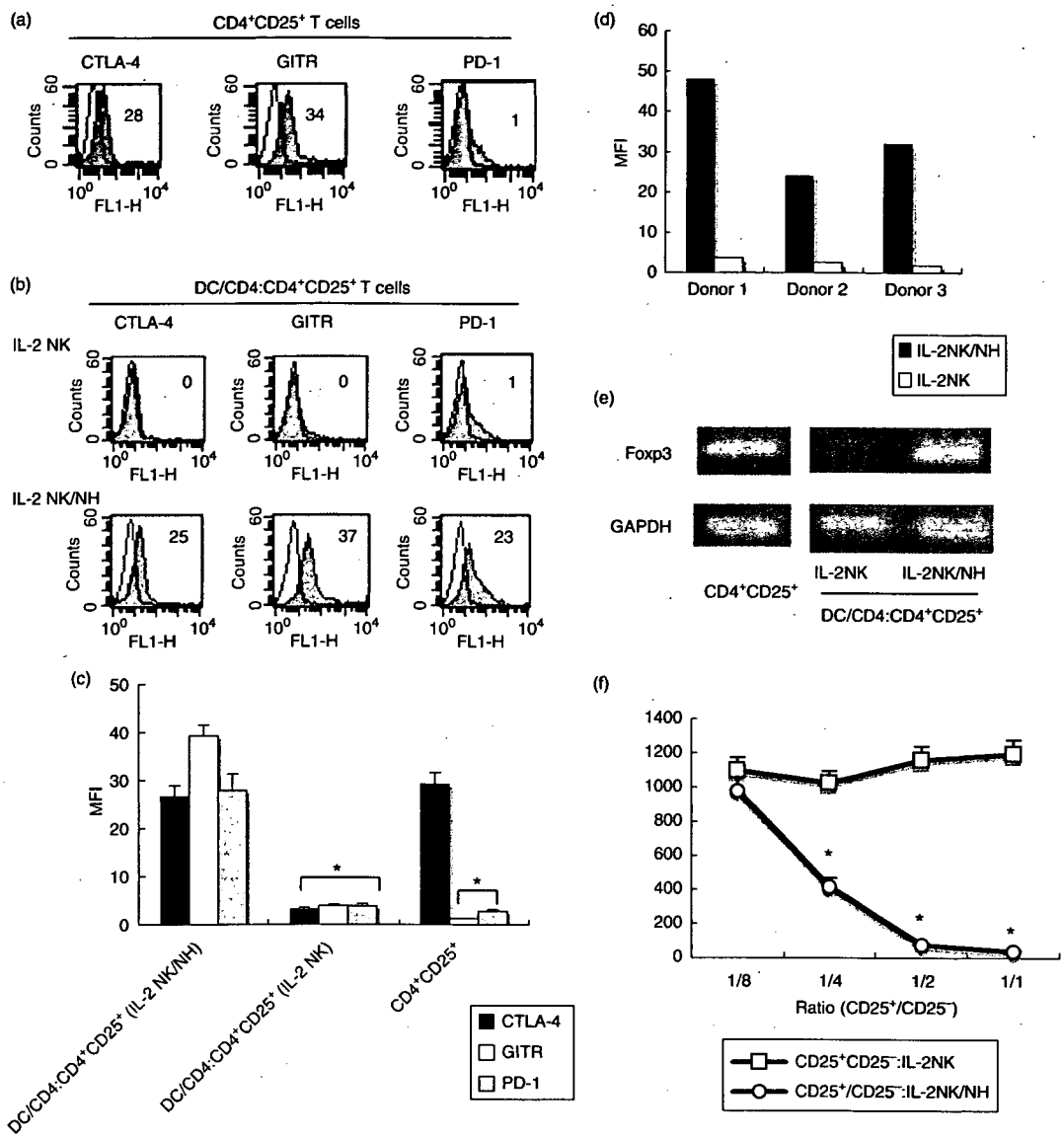

Figure 1. Human non-transformed hepatocyte (NH) modulation of activated natural killer (NK) cells endows dendritic cells (DCs) with the ability to induce $CD4^+$ $CD25^+$ regulatory T cells. (a) Freshly isolated $CD4^+$ $CD25^+$ T cells were cultured in the presence of plate-bound anti-CD3 antibody (Ab) for 24 hr, and then subjected to flow cytometry to examine their expression of cytotoxic T lymphocyte antigen-4 (CTLA-4), glucocorticoid-induced TNF receptor (GITR) and programmed death-1 (PD-1) (closed histograms). Open histograms represent the staining of control Ab. Numbers on the upper right indicate the mean fluorescence intensity (MFI) of each type of stained cells. (b) NK cells were preactivated with 50 ng/ml interleukin (IL)-2, and co-cultured in the absence (IL-2 NK) or presence (IL-2 NK/NH) of NHs at a ratio of 1 : 1 for 24 hr. DCs (1×10^5) were stimulated for 24 hr with the supernatant obtained from the co-cultured medium. After washing three times, DCs were cultured with allogeneic $CD4^+$ T cells for 48 hr. $CD4^+$ $CD25^+$ fractions were isolated from the DC/$CD4^+$ T co-culture and subjected to flow cytometry for expression of CTLA-4, GITR or PD-1 (closed histograms). Open histograms show isotype control staining. Numbers on the upper right indicate the MFI of each type of stained cell. (c) All experiments in (a) and (b) were performed three times and the composite results with statistical analysis are shown as the MFI of the staining cells. $^*P < 0{\cdot}05$ vs. responses of IL-2 NK/NH group. The experiment was performed with a different set of donors and similar results were obtained. (d) PD-1 expression on $CD4^+$ $CD25^+$ T cells stimulated with allogeneic DCs from three different donors, shown as the MFI. (e) $CD4^+$ $CD25^+$ T cells were prepared as described above. The mRNA expression of Foxp3 and GAPDH (glyceraldehyde 3-phosphate dehydrogenase) was examined by reverse transcription-polymerase chain reaction (RT-PCR). (f) $CD4^+$ $CD25^+$ fractions were isolated from DC/$CD4^+$ T cell co-cultures. Different numbers of these $CD4^+$ $CD25^+$ T cells were co-cultured with freshly isolated autologous $CD4^+$ $CD25^-$ T cells (1×10^5/well) in the presence of plate-bound anti-CD3 Ab ($CD4^+$ $CD25^+$/$CD4^+$ $CD25^-$). The anti-CD3 Ab-activated $CD4^+$ $CD25^-$ T cells alone were used as a positive control ($CD4^+$ $CD25^-$). IFN-γ was measured for each supernatant obtained after 48 hr of co-culture by enzyme-linked immunosorbent assay. $^*P < 0{\cdot}05$.

stimulated with IL-2 NK-primed DCs for 24 hr, Foxp3 was not expressed on $CD4^+$ $CD25^+$ T cells. By contrast, they dominantly transcribed Foxp3 at levels comparable with those of natural $CD4^+$ $CD25^+$ T cells when stimulated with NH/IL-2 NK-primed DCs (Fig. 1e). Taken together, $CD4^+$ $CD25^+$ T cells, when stimulated by NH/IL-2 NK-primed DCs, maintained regulatory phenotypes such as CTLA-4, GITR and Foxp3, and properties distinct from those of natural $CD4^+$ $CD25^+$ Treg cells in terms of PD-1 expression.

$CD4^+$ $CD25^+$ T cells on stimulation of NH/IL-2 NK-primed DC suppressed effector cell functions

We next analysed the functions of $CD4^+$ $CD25^+$ T cells stimulated by NH/IL-2 NK-primed DC. $CD4^+$ $CD25^+$ T cells were co-cultured for 72 hr with $CD4^+$ $CD25^-$ T cells freshly isolated from the same donors. During the co-cultures, $CD4^+$ $CD25^-$ T cells were stimulated with plate-bound anti-CD3 Ab. The $CD4^+$ $CD25^+$ T cells induced by NH/IL-2 NK-primed DCs dose-dependently suppressed the proliferation of co-cultured cells, whereas those induced by IL-2 NK-primed DC did not (data not shown). $CD4^+$ $CD25^+$ T cells induced by NH/IL-2 NK-primed DCs also dose-dependently inhibited IFN-γ production of the co-cultured cells, by contrast with those induced by IL-2 NK-primed DCs (Fig. 1f). The suppressive activities of these $CD4^+$ $CD25^+$ Treg cells were similar to those of natural $CD4^+$ $CD25^+$ Treg cells (data not shown). These results demonstrate that $CD4^+$ $CD25^+$ T cells induced by NH/IL-2 NK-primed DCs exert suppressive actions to effector cell functions, consistent with their expression of regulatory markers. Taken together, these results indicated that NK cell modulation of DCs leads to the $CD4^+$ $CD25^+$ Treg cell-mediated suppression of effector cell responses when NK cells encounter hepatocytes.

NKG2A signal of NK cells is responsible for the modulation of DCs to activate $CD4^+$ $CD25^+$ Treg cells

We examined the expression of various ligands for NK cell receptors on NHs. NHs expressed HLA-E, the ligand of NKG2A, but did not express NKG2D receptor ligands, MIC and ULBP1-2 (Fig. 2a). Given our previous findings that NHs negatively regulated IL-2 NK-mediated modulation of DC functions through the interaction of the NKG2A inhibitory receptor and its ligand HLA-E,[20] we evaluated the role of these receptor signals in the induction of $CD4^+$ $CD25^+$ Treg cells by DCs. When anti-NKG2A Ab was added during the co-culture of NH and IL-2 NK and DCs were stimulated with the resultant supernatant, the expression of CTLA-4, GITR and PD-1 was diminished on $CD4^+$ $CD25^+$ T cells (Fig. 2b, c). NKG2A blockade also suppressed PD-1 expression on $CD4^+$ $CD25^+$ T cells stimulated with IL-2NK/NH-primed DCs from three different donors (Fig. 2d). The anti-NKG2A neutralizing Ab treatment also abrogated Foxp3 expression in $CD4^+$ $CD25^+$ Treg cells (Fig. 2e). Moreover, the blockade of NKG2A signals during NH and IL-2 NK co-cultures resulted in inhibition of the DC ability to induce $CD4^+$ $CD25^+$ T cells with regulatory functions; these $CD4^+$ $CD25^+$ T cells did not suppress proliferation or IFN-γ production (Fig. 2f and data not shown) of $CD4^+$ $CD25^-$ T cells. Altogether, the activation of NKG2A inhibitory signals during NK cell and hepatocyte interaction was required for the DC induction of $CD4^+$ $CD25^+$ T cells with regulatory phenotypes and functions.

Change of cytokine milieu, triggered by NKG2A signals, plays a critical role in DC-mediated induction of $CD4^+$ $CD25^+$ Treg cells

TNF-α has been well known as a critical factor for NK cell-mediated maturation of DCs.[27] By contrast, IL-10 and TGF-β are known to act as suppressive factors of effector immune responses, and their roles in modulating DCs for Treg cell induction has recently been validated.[12–14] These findings led us to evaluate the change in cytokine production patterns in NH and IL-2 NK co-cultures in the presence or absence of anti-NKG2A Ab. ELISA data showed that the production of IFN-γ and TNF-α from NH and IL-2 NK co-cultures were substantially increased in the presence of anti-NKG2A Ab. By contrast, the addition of NKG2A masking Ab during the co-culture resulted in the marked reduction of IL-10 and TGF-β from co-cultured cells (Fig. 3a).

We next examined whether these changes of cytokine profiles were responsible for the DC induction of the $CD4^+$ $CD25^+$ Treg cells. For this purpose, the NH and IL-2 NK co-culture supernatant was treated with neutralizing Ab of IL-10 or TGF-β before DC stimulation, and suppressive activity was evaluated by analysing $CD4^+$ $CD25^+$ T cells obtained from $CD4^+$ and DC mixtures. The neutralization of IL-10 did not reverse the suppressive actions of $CD4^+$ $CD25^+$ Treg cells, but the blockade of TGF-β led to reversal of $CD4^+$ $CD25^+$ Treg cell activities (Fig. 3b).

We directly examined the effect of TGF-β on the modulation of DC ability to induce $CD4^+$ $CD25^+$ Treg cells. TGF-β endowed DCs with the ability to induce $CD4^+$ $CD25^+$ Treg cells. TNF-α inhibited TGF-β-mediated DC induction of $CD4^+$ $CD25^+$ Treg cells (Fig. 3c). By contrast, IFN-γ had little effect on the modulation of DC by TGF-β (data not shown). Taken together, these results strongly suggest that increased TGF-β and decreased TNF-α production, the change of cytokine profiles mediated by the NKG2A signals, are involved in DC-mediated $CD4^+$ $CD25^+$ Treg cell induction.